Progress In Electromagnetics Research C, Vol. 135, 69–81, 2023

A Folded Rectenna on a Flexible Substrate for 5G Energy Harvesting Applications

Mustapha Bajtaoui*, Mohammed A. Ennasar, Mariem Aznabet, Abdelmounaim Tachrifat, and Otman EL Mrabet

Abstract—This paper presents the design, fabrication, and measurement results of a flexible folded dipole rectenna for 5G technology. The proposed rectenna is a single-sided structure fabricated on a flexible Kapton substrate with a maximum RF to DC conversion efficiency close to 53% for an input power of −9 dBm at 3.5 GHz with 3-kΩ. Moreover, the measured results show that the conversion efficiency is above 40% across a broad range of input power levels (from −14 to −8 dBm). The paper discusses the prototype's design and simulation results, fabrication steps, and measurement results. The proposed rectenna is compact, low-cost, and flexible, making it suitable for wearable applications.

1. INTRODUCTION

In the last decade, flexible and wearable devices have gained much attention among researchers and scientists [1, 2]. Nowadays, these devices have been embedded in many aspects of our daily lives, including electronic skin (e-skin) and health monitoring sensors [3–5]. By 2025, internet of things (IoT) analytics expects more than 20 billion devices to be deployed worldwide [6]. This rapid development leads to the use of a considerable number of batteries. Therefore, the design of self-sustained wearable electronic devices is highly appealing. One way to overcome the problem of the energy supply issue in wearable electronics is to harvest ambient energy from the environment, known as electromagnetic energy harvesting. The main challenge of energy harvesting and wireless power transfer is that the available ambient RF power density is very low. Hence, the harvested DC voltage cannot supply the low-power IoT nodes. However, the fifth generation (5G) of mobile communications provides a powerful source of ambient energy, which has transformed the base station into a powerful source of electromagnetic waves and can serve as a helpful wireless power grid [7].

In contrast, the Federal Communication Commission (FCC) has increased the permitted equivalent isotropic radiated power (EIRP) in the mm-wave 5G band (> 24 GHz) beyond 75 dBm at 100 meters from the transmitter in comparison to the 3-G and 4-G frequency bands. The fifth generation (5G) band is between 3.4 and 3.8 GHz, with bandwidth more significant than the one reserved for 4G technology. Thus, to cover the same area as in 4G, an increase in bandwidth requires an increase in power by the same factor. This opens the possibility of powering low-power IoT devices from different distances.

A few initial factors should be considered while an appropriate rectenna is designed for wearable electronics devices used in IoT, smart cities, and innovative health applications, to name a few. For example, the rectenna should be low profile, low-cost, flexible, comfortable, and conformal to the body shape. Several wearable rectennas printed on a flexible substrate (such as Kapton) or a textile substrate [8–16] have been reported in the literature. For example, the authors in [12] presented a new dual-band flexible rectenna with a cylindrical shape capable of harvesting energy from various RF

Received 15 May 2023, Accepted 8 July 2023, Scheduled 25 July 2023

* Corresponding author: Mustapha Bajtaoui (mustaphabajtaoui@gmail.com).

The authors are with the Information and Telecommunication System Laboratory (LaSiT), Faculty of Science, Abdelmalek Essaadi University, Tétouan 93000, Morocco.

sources (LTE 1.8 GHz and Wi-Fi 2.45 GHz) available across the entire azimuth plane. The measured results show that the fabricated prototype consists of a single rectenna unit that can convert power with 40% efficiency at a meager input RF power of −12 dBm. For the same field of applications, authors in [10] developed textile rectenna arrays for powering wearable electronic devices. It was found that when the Wi-Fi ambient signal was amplified using an external amplifier, the fabricated 2×2 rectenna-array system demonstrated a peak dc power up to 100 µW under natural ambient power collection conditions. The 2×3 array delivered the average dc power up to 600 µW at 10 cm and 80 µW at 60 cm from the source.

This paper uses a flexible folded dipole rectenna working at 3.5 GHz for 5G, which is designed, fabricated, and measured. The proposed rectenna is manufactured on one side of an adhesive, flexible, and resistant substrate of Kapton polyimide thin film, which allows it to conform to different objects, enabling seamless integration into a wide range of devices. This flexibility expands the horizons of energy harvesting, opening up possibilities for applications in areas such as wearable electronics and IoT devices. The Schottky diode (SMS7630079LF) is directly connected with the dipole antenna without using a matching network, making its dimension compact. The conjugate matching between the dipole antenna and the diode is achieved by adjusting the parameter of the slots inserted into the dipole antenna. The rest of this paper is organized as follows. The second section presents and discusses the design and simulation results of the flexible folded rectenna. Next, the fabrication steps and measurements result of the fabricated prototype are given in Section 3. Finally, the conclusion of this paper is provided in the last section.

2. INPUT IMPEDANCE OF THE RECTIFIER DIODE

Generally, when a rectenna is designed, the main parts, which are rectifier and antenna, are designed separately, then connected via a matching network. In contrast, in this paper, the proposed flexible folded dipole rectenna is designed with integrated impedance matching. Thus, a conjugate matching between the diode and the folded dipole antenna is needed to achieve maximum power transfer. This condition can be observed by calculating the reflection coefficient using the following equation:

$$\Gamma = \frac{Za - Zd^*}{Za + Zd^*} \tag{1}$$

where Z_a represents the impedance of the antenna, and Z_d^* is the complex conjugate of the diode impedance. In this work, the rectifier uses a Skyworks SMS7630-079LF zero-bias Schottky diode in a SOT-23 package, which is most appropriate for low RF input power applications. This Schottky diode has minor parasitic effects modeled by a capacitance in parallel circular polarization (CP) and an inductance linear polarization (LP) in series, and their values are 0.185 pF and 0.7 nH, respectively. The designed antenna topology is a folded dipole antenna printed on a DuPontTM Kapton polyimide flexible substrate [17] having a thickness of 0.127 mm, dielectric constant of 3.5, and loss tangent of 0.002. The dielectric constant of this substrate has been obtained using the coaxial probe method [18, 19]. More information about the properties of this material can be found in [20].

To investigate the proposed rectenna's operating characteristics, the diode's input impedance was calculated using a commercial simulator called Advanced Design System (ADS). In general, the input impedance of the Schottky diode varies when the input power is changed. This variation can be ascribed to the fact that the junction capacitance depends on the voltage across the Schottky diode. The ADS simulator provides two different kinds of simulations that can be used for input impedance analysis of the Schottky diode. The first one is called Large Signal S-parameter (LSSP) simulation, which allows getting the reflection coefficient and then input impedance. The second one is Harmonic Balance (HB) simulation which enables us to estimate the level of rectified DC component, fundamental frequency, and its harmonics at the rectifying circuit's output, respectively.

In this paper, an LSSP simulation, as shown in Figure 1, has been performed to estimate the input impedance of the Schottky diode at specific value of input RF power level and operating frequency.

For the simulations, the Schottky-diode model SMS7630-079LF in SOT-23 (see Figure 2) was chosen, and hence the SPICE parameters [21] are used as shown in Table 1. The input power value is chosen to be −9 dBm, and the operation frequency of 3.5 GHz is selected. Note that in our previous work published in [22], we found that the breakdown voltage (B_v) given in the datasheet was not

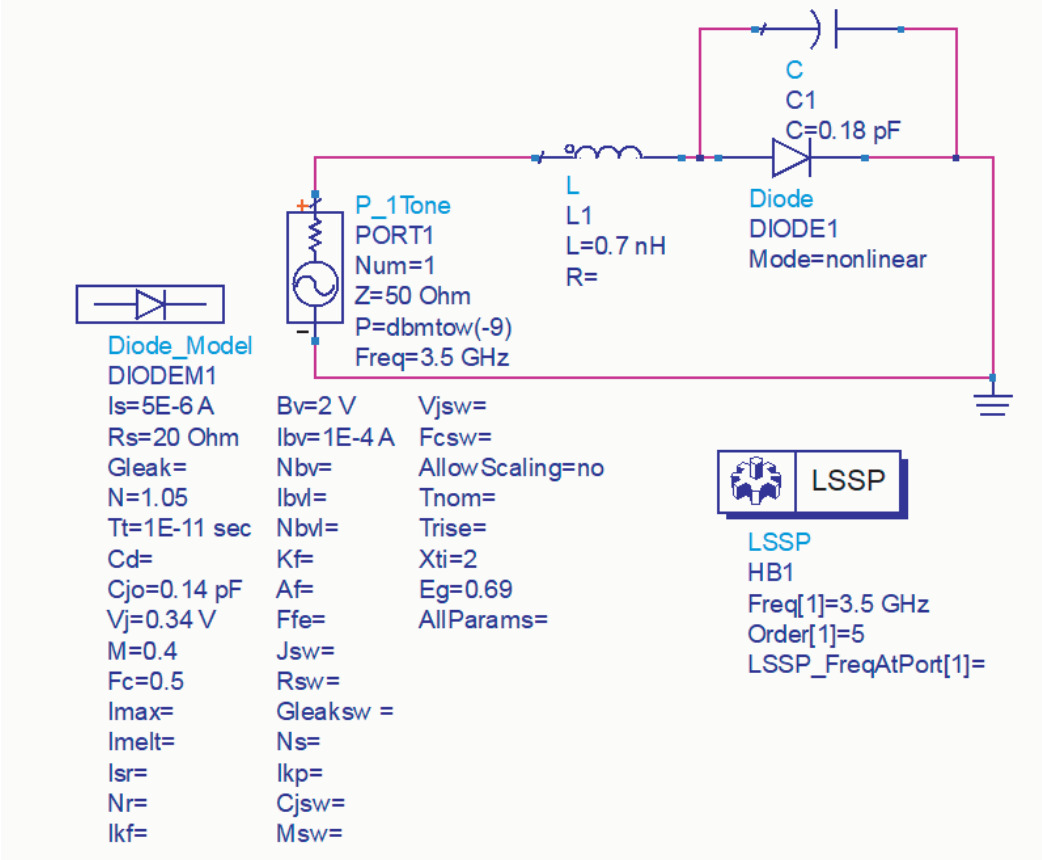

Figure 1. LSSP Simulation set-up to estimate the input impedance of the Schottky Diode SMS7630-079LF in SOT-23.

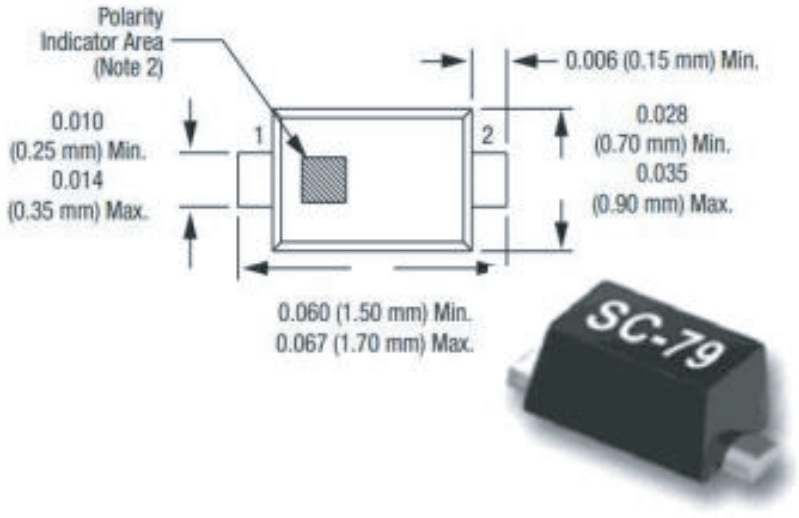

Figure 2. Photograph of the Schottky Diode SMS7630-079LF in SOT-23.

appropriate, which led to a discrepancy between the simulated and measured results [23]. A sweep of this parameter leads to an optimal value greater than the one listed in the datasheet to have a good agreement between the two data sets. For more information about this parameter, one can refer to our work published in [22].

Table 1. Spice Model of the Schottky Diode SMS7630-079LF in SOT-23.

Parametres	Units	Values
B_v	V	2
C_{j0}	pF	0.14
E_g	eV	0.69
I_{BV}	A	1.10^{-4}
I_S	A	5.10^{-6}
N		1.05
R_S	Ω	20
Vj	V	0.34
W_{Ti}		2
M		0.4

The simulation results show that the reflection coefficient S_{11} is $(0.55 - j0.532)$ at the operating frequency of 3.5 GHz. Thus, the correct input impedance of the Schottky diode can be calculated using the following equation:

$$Z_{Diode} = Z_0 \frac{1 + S_{11}}{1 - S_{11}} \tag{2}$$

where S_{11} is the reflection coefficient, Z_{Diode} the input impedance of the diode, and Z the impedance of a 50-Ω transmission line. Using Equation (2), the input impedance of the diode is equal to $Z_{Diode} = (42.701 - j109.625)\,\Omega$.

It is worth noticing that the chosen input power, which is −9 dBm, is not relatively small. Hence, Equation (2) held only for small input power may cause some inaccuracy. To check this point, the input impedance obtained above with its complex conjugate on the Smith chart is presented in Figure 3. The

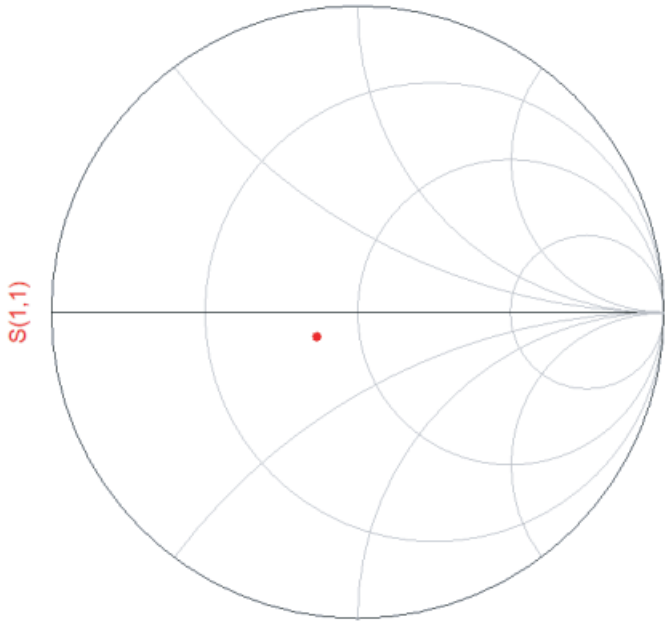

Figure 3. Impedance of the Schottky diode with an input power of −9 dBm.

impedance matching point is located near the center of the Smith chart, indicating that there needs to be a better match between the diode's input impedance and its complex impedance. This mismatch can be ascribed to the nonlinear behavior of the Schottky diode raised by the junction capacitance C_j. Thus, a tuning process must be performed to find the exact value of the input impedance of the Schottky diode that leads to maximum power transfer.

After careful tuning, the input impedance of the Schottky diode that enables a maximum power transfer was found to be $Z_{Diode} = (26.2 - j122)\,\Omega$. The input impedance of the Schottky diode is capacitive and, therefore, needs an inductive dipole antenna to get a good conjugate matching with the Diode.

3. FLEXIBLE FOLDED DIPOLE ANTENNA TOPOLOGY

The proposed flexible folded dipole antenna without the rectifying part was designed and optimized using the electromagnetic software CST Microwave Studio, a commercial tool based on the Finite Integration Method (FIT) [24]. Note that the same design was reported previously in [25] with a rigid substrate and working at 2.45 GHz. The configuration of the proposed structure is shown in Figure 4. This antenna consists of two symmetrical capacitive arms to achieve a compact design. The two arms are separated at the center using two different gaps, W_2 and W_3.

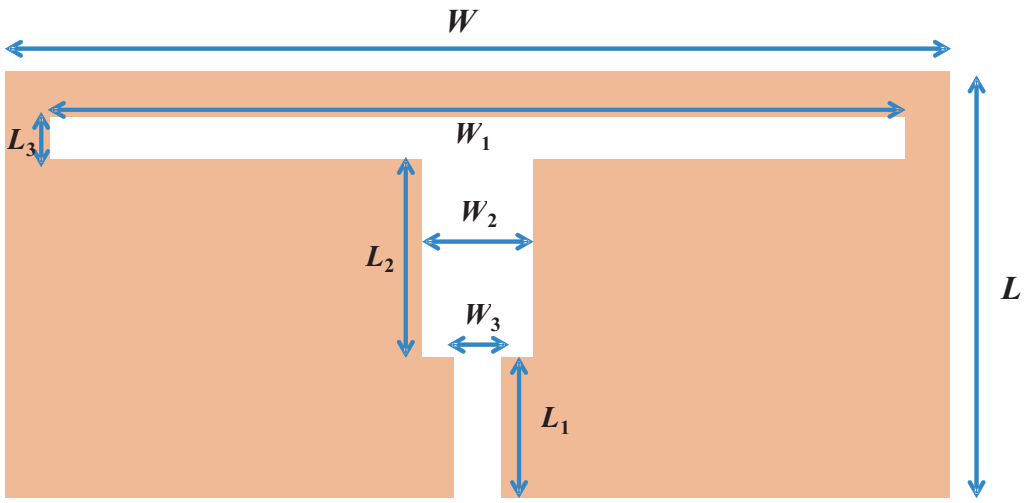

Figure 4. Configuration of the proposed flexible dipole antenna.

Some slots are introduced in the proposed design to get a good conjugate impedance matching with the Schottky diode. The 50-Ω port is placed across the gap W_3 between the two arms, as shown in Figure 4. As mentioned, the proposed dipole antenna is printed on a DuPontTM Kapton polyimide flexible substrate with a thickness of 0.127 mm, dielectric constant of 3.5, and dielectric loss tangent of 0.002. All geometrical parameters of this folded antenna (after optimization to be discussed later) are listed in Table 2.

Table 2. Optimized geometrical parameters of the proposed folded dipole antenna.

Width	Value (mm)	length	Value (mm)
W	70	L	25
W_1	59.6	L_1	10
W_2	8	L_2	12
W_3	1	L_3	1

To maximize the received energy from an incident wave, the folded dipole antenna dimensions were optimized to match the conjugate of the diode impedance Z_{Diode}. Due to the highly capacitive input impedance of the rectifying diode, an inductive dipole antenna is required to provide good conjugate matching. A full wave simulator CST Microwave Studio (CST) was used to optimize the proposed structure to work at the operating frequency of 3.5 GHz. For the sake of brevity, many simulations not shown here have been performed. It is found that the main parameter that significantly influences the input impedance of the antenna (real and imaginary part) is the length W_1 of the biggest slot, see Figure 4. Figure 5 shows the simulated input impedance of the folded antenna for different values of W_1 as a function of frequency.

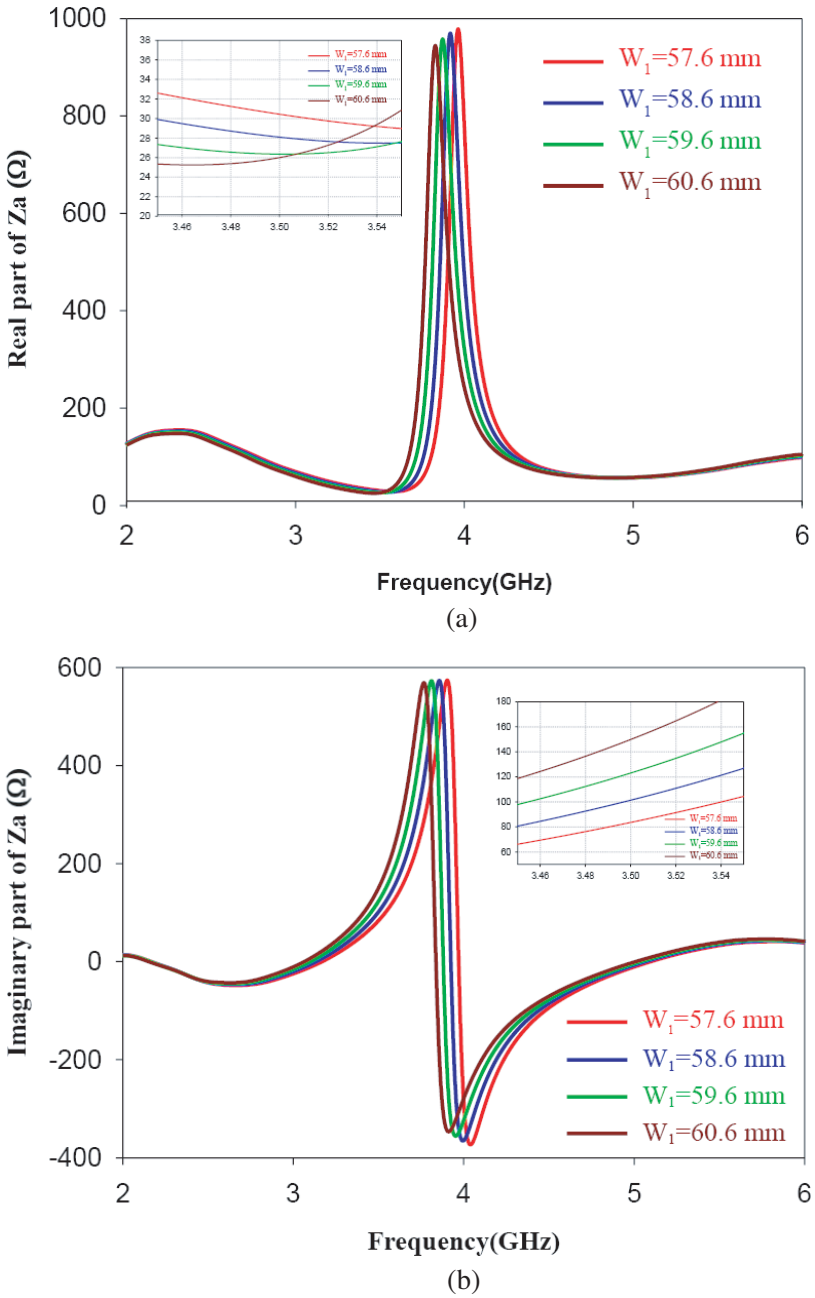

Figure 5. Simulated input impedance Z_a of the designed folded antenna for different values of W_1. (a) real part; (b) imaginary part.

It should be noted that when one parameter is changed, the other parameters indicated in Table 2 remain unchanged. Figure 5 reveals that parameter W_1 can also control the resonance frequency of the folded antenna. Higher resonance frequencies result from small variations of the parameter (W_1) because the effective length of the antenna's arm is shorter. The inset of Figure 5 provides more information on the variation of the real and imaginary parts of the input impedance Z_a of the antenna with parameter W_1 around the operating frequency of 3.5 GHz. The effect of this parameter W_1 on the imaginary parts of the input impedance is far less than the influence introduced in the real part. This characteristic allows for the optimization of the real and imaginary parts of the antenna to be in conjugate match with the Schottky diode impedance. Indeed, for W_1 equal to 59.5 mm, the input impedance of the folded antenna is $Z_a = (26.822 + j120.332)\,\Omega$.

From the above results, the reflection coefficient can be calculated. The obtained results are depicted in Figure 6. The proposed structure has a resonance frequency of around 3.5 GHz with a good impedance matching less than -40 dB.

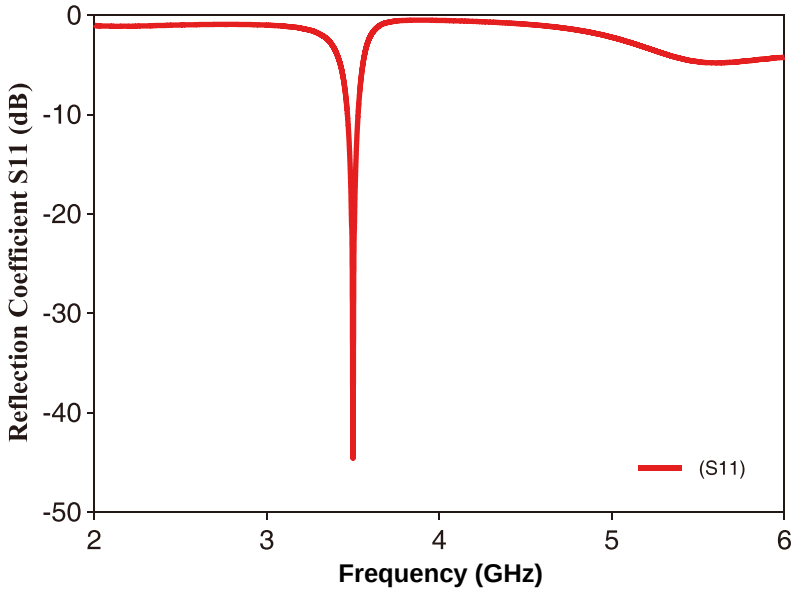

Figure 6. Simulated reflection coefficient of the folded antenna.

The antenna gain, a crucial parameter for rectenna, has also been simulated. The obtained results shown in Figure 7 reveal that the proposed design has a gain close to 6 dB.

Before going to the fabrication process, the effect of adding a resistor and capacitor on the input impedance of the designed folded antenna has been studied. To introduce the latter components inside the antenna minor modifications to the first design shown in Figure 4 have been made. The new configuration of our design that integrates the capacitor ($C = 100$ pF) and the resistor ($R = 3\,\text{k}\Omega$) is shown in Figure 8.

The simulated results regarding the input impedance as a function of frequency presented in Figure 9 show that introducing the capacitor and resistor does not affect the input impedance. This can be explained by the fact that the capacitor behaves as a short circuit at the operating frequency (3.5 GHz).

The effect of different resistor (R_{Load}) values on the reflection coefficient has been numerically investigated. The results presented in Figure 10 show that the reflection coefficient remains unchanged with the variation of R_{Load}.

4. FLEXIBLE FOLDED DIPOLE RECTENNA

A prototype of the proposed flexible folded rectenna has been fabricated and tested. Note that the prototype shown in Figure 11 is fabricated using the following process, which can be divided into

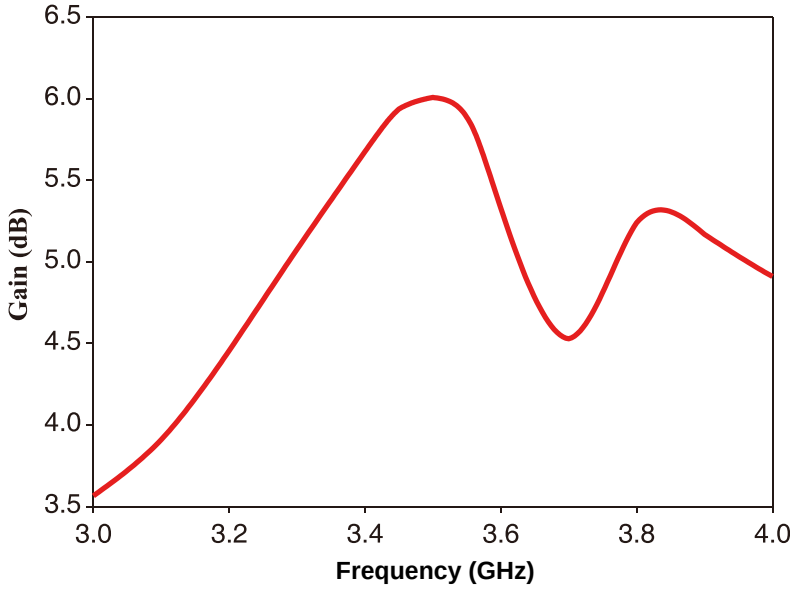

Figure 7. Simulated gain of the folded antenna.

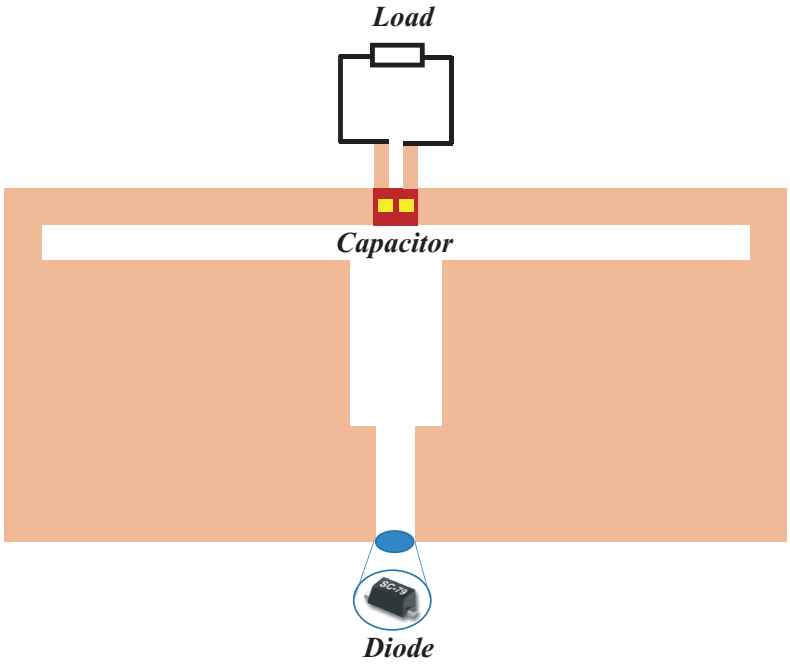

Figure 8. The new configuration of the folded antenna with integrated resistor and capacitor.

different steps. First, a mask that incorporates the complementary shape of the rectenna is created. The mask has then been adhered to a thin copper layer sheet. Cu etchant is used to remove the copper from the undesirable area so that the configuration rectenna top layer can be reproduced. The latter is washed with isopropyl alcohol and rinsed with deionized water before immediately bonding to the flexible Kapton polyimide substrate.

It is important to note that the main blocks of a rectenna (antenna and rectifier) are designed independently. The primary benefit of this strategy is that it gives you a clear understanding of how each block performs and makes it possible to spot any issues that need to be resolved before fabricating the final prototype. In contrast, in our case, the folded antenna has an integrated rectifier allowing us

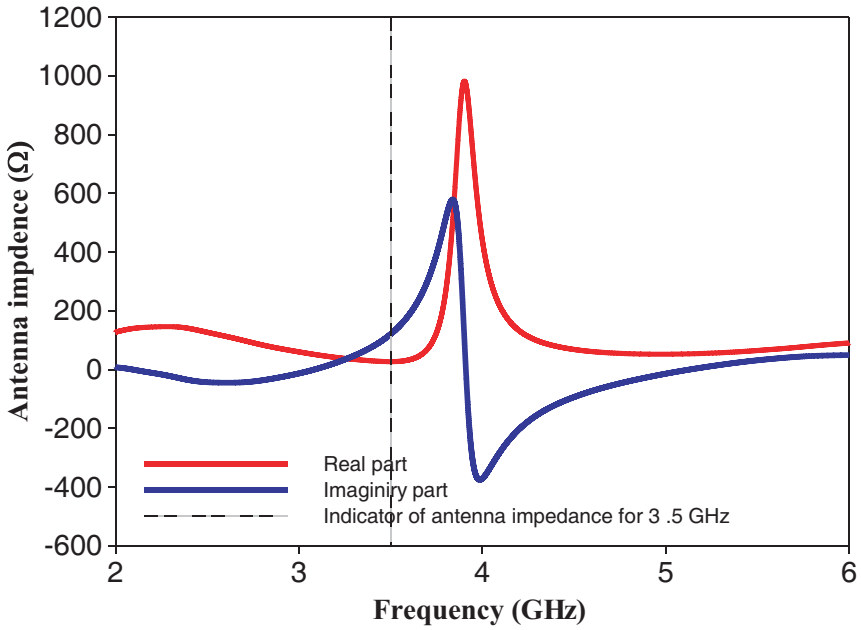

Figure 9. Simulated input impedance Za of the designed folded antenna with the integration of the capacitor and resistor.

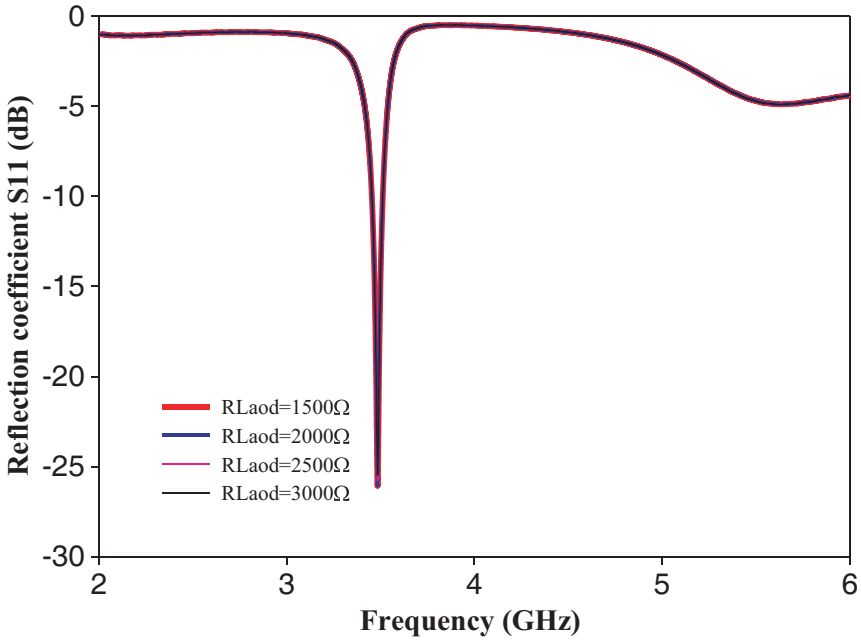

Figure 10. Simulated reflection coefficient for different values of R_{Load}.

to have a compact design.

The flexible folded rectenna was measured in free space using the measurement setup shown in Figure 12. It consists of an ultra-wideband (UWB) Double-Ridged TEM linear polarized horn antenna with lens (2 GHz–26 GHz) to emit the electromagnetic power generated from an RF signal source from Rhode Schwartz to the rectenna. The realized gain of this linearly polarized horn antenna is approximately 10 dBi at 3.5 GHz. The LP horn antenna is connected to an RF signal source via a coaxial cable having a total loss of 2 dB at 3.5 GHz. The rectenna was placed 0.5 m away from the LP

Figure 11. A photo of the fabricated prototype of the proposed rectenna.

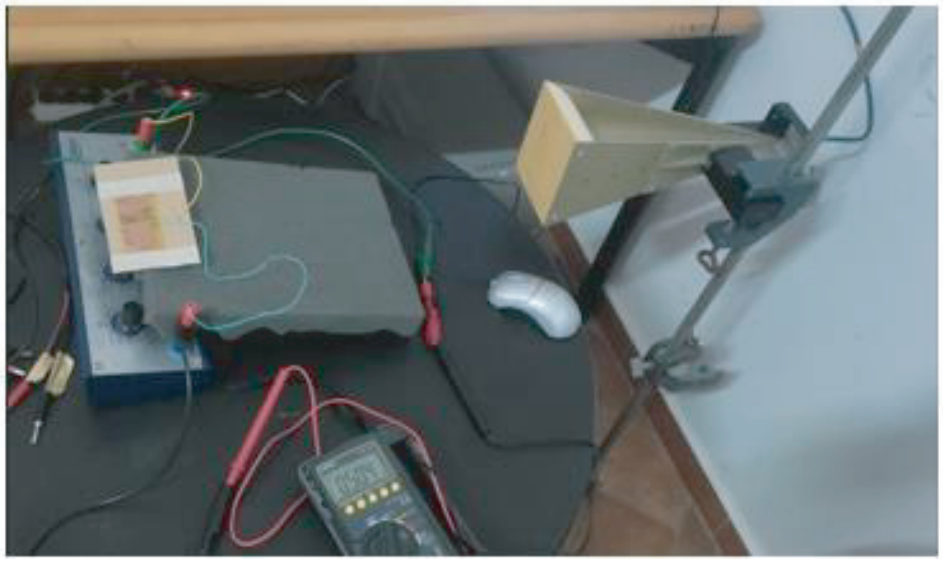

Figure 12. Measurement set-up in free space.

horn antenna, which is in the far-field region of the LP horn antenna. The output dc voltage V_{out} of the rectenna was measured with a multimeter.

First, the output voltage V_{DC} (across the load resistance R_{Load}) as a function of input power at 3.5 GHz, as shown in Figure 13, has been measured. It is found that when the input power level is -9 dBm with a load of 3 kΩ, V_{DC} is close to 0.5 V.

Next, Equation (3) was used to calculate the rectenna's efficiency based on the above results. The rectenna efficiency with a load of 3 kΩ at 3.5 GHz is plotted as a function of input power level (P_{in}) in Figure 14.

$$\eta = \frac{P_{DC_{out}}}{P_{RF_{in}}} * 100 = \frac{V_{out}^2}{R_{DC}} * \frac{1}{P_{RF_{in}}} * 100 \tag{3}$$

When the P_{in} is -9 dBm, the rectenna has an efficiency around 53%. Note that the measured efficiency is above 40% in a wide range of input power levels (from -14 to -8 dBm).

Table 3 compares the flexibility, size, and conversion efficiency of our proposed flexible rectenna compared to the previous designs reported in the literature. Comparing the proposed flexible rectenna to the designs listed in Table 3, it is clear that the proposed design has a higher conversion efficiency while being smaller in size.

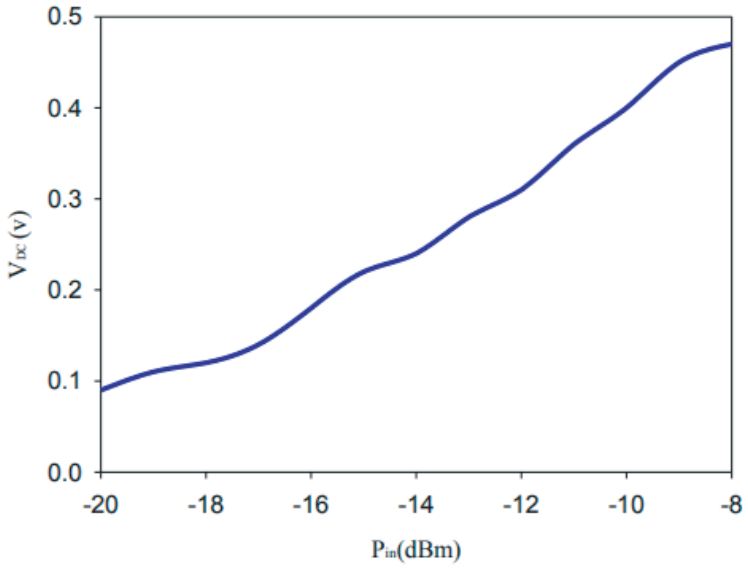

Figure 13. Measured output voltage V_{DC} as a function of the input power level at 3.5 GHz.

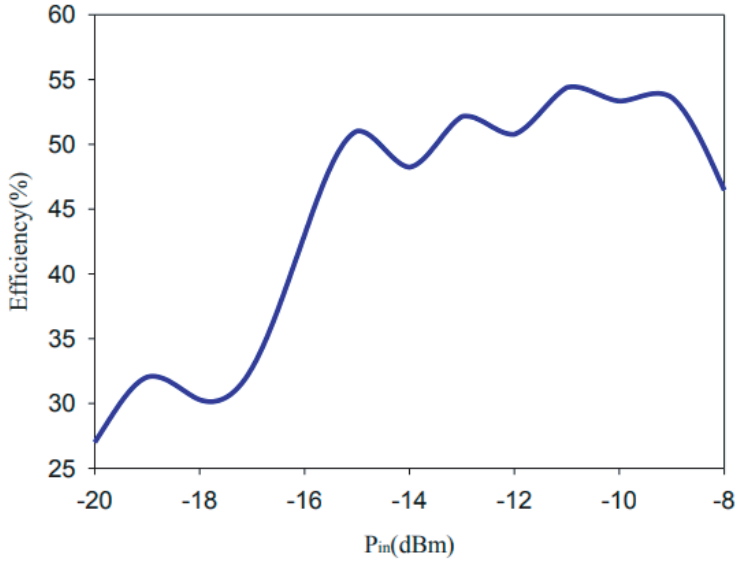

Figure 14. Measured efficiency of the rectenna as a function of the input power level at 3.5 GHz.

Table 3. Comparison of the flexible rectenna with other published rectennas.

Ref.	Freq. (GHz)	Eff @ Pin_{opt}	Flexibility	Size (mm^2)
[7]	0.86–0.916	50	yes	190 × 139
[22]	2.4–2.45	46	No	114 × 40
[26]	0.8–0.9; 1.8–1.9	15	Yes	130 × 130
[27]	2.4–2.5	28	Yes	49 × 54
[28]	2.45	41.63	No	60 × 80
This work	3.5	53	Yes	70 × 30

5. CONCLUSION

In summary, this study discusses the design, fabrication, and testing of a compact rectenna working at 3.5 GHz. By integrating the rectifying diode (SMS7630-079LF) into a flexible folded antenna, a compact, flexible, and integrated battery-free rectenna, with a whole dimension of $70 \times 30\,\mathrm{mm}^2$, which can wirelessly harvest electromagnetic waves in the band of 5th Generation (5G), has been successfully demonstrated. The measured results show that dc voltage (V_{DC}) at 3.5 GHz is near 0.5 V, and the resulting conversion efficiency is close to 53% with an input power level of −9 dBm when it is terminated with a load of 3 kΩ. The measured results also show that the conversion efficiency remains above 45% in a wide range of input power levels (from −14 to −8 dBm). This work represents a critical breakthrough for fabricating a flexible design that may hold promise for wirelessly powering IoT devices using the existing 5G infrastructure as an energy power grid.

REFERENCES

1. Gu, Y., T. Zhang, H. Chen, et al., "Mini review on flexible and wearable electronics for monitoring human health information," *Nanoscale Res. Lett.*, Vol. 14, 263, 2019.
2. Seshadri, D. R., J. R. Rowbottom, C. Drummond, J. E. Voos, and J. Craker, "A review of wearable technology: Moving beyond the hype: From need through sensor implementation," *2016 8th Cairo International Biomedical Engineering Conference (CIBEC)*, 52–55, 2016.
3. Ates, H. C., P. Q. Nguyen, L. Gonzalez-Macia, et al., "End-to-end design of wearable sensors," *Nat. Rev. Mater.*, Vol. 7, 887–907, 2022.
4. Vijayan, V., J. P. Connolly, J. Condell, N. McKelvey, and P. Gardiner, "Review of wearable devices and data collection considerations for connected health," *Sensors (Basel).*, Vol. 21, No. 16, 5589, 2021.
5. Iqbal, S. M. A., I. Mahgoub, E. Du, et al., "Advances in healthcare wearable devices," *NPJ Flex Electron*, Vol. 5, 9, 2021.
6. https://iot-analytics.com/number-connected-iot-devices/.
7. Monti, G., L. Corchia, and L. Tarricone, "UHF wearable rectenna on textile materials," *IEEE Transactions on Antennas and Propagation*, Vol. 61, No. 7, 3869–3873, Jul. 2013.
8. Estrada, J., E. Kwiatkowski, A. Lopez-Yela, M. Borgonos-Garcia, D. Segovia, T. Barton, and Z. Popovic, "An octave bandwidth RF harvesting tee-shirt," *2019 IEEE Wireless Power Transfer Conference (WPTC)*, 1–4, Jun. 2019.
9. Eid, A., J. G. Hester, and M. M. Tentzeris, "5G as a wireless power grid," *Sci. Rep.*, Vol. 11, No. 1, 1–9, 2021.
10. Vital, D., S. Bhardwaj, and J. L. Volakis, "Textile-based large area RF-power harvesting system for wearable applications," *IEEE Transactions on Antennas and Propagation*, Vol. 68, No. 3, 2323–2331, Mar. 2020.
11. Wagih, M., N. Hillier, S. Yong, A. S. Weddell, and S. Beeby, "RF-powered wearable energy harvesting and storage module based on E-textile coplanar waveguide rectenna and supercapacitor," *IEEE Open Journal of Antennas and Propagation*, Vol. 2, 302–314, 2021.
12. Wagih, M., A. S. Weddell, and S. Beeby, "Omnidirectional dual polarized low-profile textile rectenna with over 50% efficiency for sub-$\mu W/cm^2$ wearable power harvesting," *IEEE Transactions on Antennas and Propagation*, Vol. 69, No. 5, 2522–2536, 2020.
13. Eid, A., J. Hester, A. Nauroze, et al., "A flexible compact rectenna for 2.40 Hz ISM energy harvesting applications," *2018 IEEE International Symposium on Antennas and Propagation & USNC/URSI National Radio Science Meeting*, 1887–1888, 2018.
14. Chandravanshi, S., K. K. Katare, and M. J. Akhtar, "A flexible dual-band rectenna with full azimuth coverage," *IEEE Access*, Vol. 9, 27476–27484, 2021.
15. Malik, B. T., V. Doychinov, S. A. Raza Zaidi, et al., "Flexible rectennas for wireless power transfer to wearable sensors at 24 GHz," *2019 Research, Invention, and Innovation Congress (RI2C)*, 1–5, Bangkok, Thailand, 2019, doi: 10.1109/RI2C48728.2019.89999.

16. Zhang, X., J. Grajal, J. L. Vazquez-Roy, et al., "Two-dimensional MoS_2-enabled flexible rectenna for Wi-Fi-band wireless energy harvesting," *Nature*, Vol. 566, 368–372, 2019.
17. Dupont Kapton FN, Available online: https://www.dupont.com/content/dam/Dupont2.0/Products/Electronics-and-imaging/Literature/DEC-Kapton-FN-datasheet.pdf, [(accessed on Jul. 3 2019)].
18. You, K. Y., H. K. Mun, J. Salleh, and Z. Abbas, "A small and slim coaxial probe for single rice grain moisture sensing," *Sensors*, Vol. 13, 2652–3663, 2013.
19. López-Rodríguez, P., D. Escot-Bocanegra, D. Poyatos-Martínez, and F. Weinmann, "Comparison of metal-backed free-space and open-ended coaxial probe techniques for the dielectric characterization of aeronautical composites," *Sensors*, Vol. 16, 967, 2016.
20. El Khamlichi, M., A. Alvarez Melcon, O. El Mrabet, M. A. Ennasar, and J. Hinojosa, "Flexible UHF RFID tag for blood tubes monitoring," *Sensors (Basel)*, Vol. 19, No. 22, 4903, Nov. 9, 2019, PMID: 31717601; PMCID: PMC6891293.
21. https://eu.mouser.com/datasheet/2/472/skyworks_surface_mount_schottky_diodes_200041w-1213983.pdf.
22. Bajtaoui, M., O. El Mrabet, M. A. Ennasar, and M. Khalladi, "A novel circular polarized rectenna with wide ranges of loads for wireless harvesting energy," *Progress In Electromagnetics Research M*, Vol. 106, 35–46, 2021.
23. Zeng, M., A. S. Andrenko, X. Liu, B. Zhu, Z. Li, and H.-Z. Tan, "Differential topology rectifier design for ambient wireless energy harvesting," *2016 IEEE International Conference on RFID Technology and Applications (RFID-TA)*, 97–101, Foshan, 2016.
24. CST Microwave Studio, 2020, [online] Available: www.cst.com.
25. Zhang, F., H. Nam, and J.-C. Lee, "A novel compact folded dipole architecture for 2.45 GHz rectenna application," *2009 Asia Pacific Microwave Conference*, 2766–2769, Singapore, 2009.
26. Collado, A. and A. Georgiadis, "Conformal hybrid solar and electromagnetic (EM) energy harvesting rectenna," *IEEE Trans. Circuits Syst. I, Reg. Papers*, Vol. 60, No. 8, 2225–2234, Aug. 2013.
27. Palazzi, V., C. Kalialakis, F. Alimenti, et al., "Performance analysis of a ultra-compact low-power rectenna in paper substrate for RF energy harvesting," *Proc. IEEE Topical Conf. Wireless Sensors Sensor Netw. (WiSNet)*, 65–68, Jan. 2017.
28. Kumar, D. and K. Chaudhary, "Design of differential source fed circularly polarized rectenna with embedded slots for harmonics suppression," *Progress In Electromagnetics Research C*, Vol. 84, 175–187, 2018.